Cancer Chemother Pharmacol (2008) 62:605–620
DOI 10.1007/s00280-007-0644-z

ORIGINAL ARTICLE

Inhibition by erlotinib of primary lung adenocarcinoma at an early stage in male mice

Laura K. Zerbe · Lori D. Dwyer-Nield · Jason M. Fritz · Elizabeth F. Redente · Robert J. Shroyer · Elizabeth Conklin · Shawn Kane · Chris Tucker · S. Gail Eckhardt · Daniel L. Gustafson · Kenneth K. Iwata · Alvin M. Malkinson

Received: 24 August 2007 / Accepted: 1 November 2007 / Published online: 21 November 2007

Abstract
Purpose Erlotinib, a small molecule inhibitor of the tyrosine kinase (TK) domain of epidermal growth factor receptor (EGFR), increases survival of advanced non-small cell lung cancer patients who failed standard chemotherapy (Phase III study). We evaluated whether erlotinib is also effective at an early stage of primary lung tumorigenesis in a carcinogen-induced lung tumor model in mice.
Methods Sixteen weeks after carcinogen (urethane) injection, when small self-contained adenomas are evident, male and female A/J mice were treated IP with 10 mg/kg erlotinib or Captisol vehicle daily over 3.5 weeks (15 mice per group). The efficacy, metabolism and mechanism of action of erlotinib were evaluated.
Results Erlotinib reduced tumor burden in males by twofold compared to vehicle (12.7 ± 1.2 vs 26.2 ± 2.5 mg, respectively; $p < 0.0001$), while tumor burden in erlotinib-treated females slightly increased compared to vehicle by 21% (15.1 ± 1.2 vs 11.9 ± 0.9 mg, respectively; $p < 0.05$). Tumor multiplicity, in contrast, was unaffected by erlotinib. The levels of erlotinib that accumulated in plasma, lung tumor tissue and adjacent uninvolved (UI) lung were comparable in males and females. Males, however, accumulated more OSI-420, an active and pharmacologically equipotent metabolite of erlotinib, than females in plasma, lung tumors, and UI lung. In both genders, 80% of tumors contained *Kras* mutations at codon 61, but no *EGFR* mutations were detected. The cellular distribution and concentration of EGFR were also similar between genders. In control mice, however, phosphorylated EGFR (pEGFR) levels were nearly 2.5-fold higher in males compared to females in UI lungs and sevenfold higher in lung tumors. Further, erlotinib decreased the contents of pEGFR in UI lungs and lung tumors, particularly in males.
Conclusions Adenomas from male mice in this early lung cancer model are responsive to erlotinib treatment, possibly because of a greater dependence of male tumor growth on the EGFR pathway compared to females. Importantly, these results indicate that small lung adenomas from male mice that utilize EGFR signaling but also harbor *Kras* mutations shrink in response to erlotinib, suggesting that erlotinib may be beneficial for some patients very early during lung cancer progression.

Keywords Erlotinib · Early-stage lung cancer · Primary mouse lung tumor model

Grant Support: USPHS grants CA33497, CA96133 and Lung Cancer SPORE P50 CA58187.

L. K. Zerbe · L. D. Dwyer-Nield · J. M. Fritz · E. F. Redente · R. J. Shroyer · A. M. Malkinson (✉)
Department of Pharmaceutical Sciences,
University of Colorado at Denver and Health Sciences Center,
4200 East Ninth Avenue, Box C238, Denver, CO 80262, USA
e-mail: al.malkinson@UCHSC.edu

E. Conklin · S. Kane · C. Tucker
OSI Pharmaceuticals Inc., Boulder, CO, USA

S. G. Eckhardt
Division of Medical Oncology,
University of Colorado at Denver and Health Sciences Center,
Denver, CO, USA

D. L. Gustafson
Department of Clinical Sciences,
Colorado State University, Fort Collins, CO, USA

K. K. Iwata
OSI Pharmaceuticals Inc., Melville, NY, USA

Introduction

Lung cancer is the most common cause of death from cancer worldwide, with 1.18 million deaths, or 17.6% of the world total [1]. In the United States, lung cancer accounts for most cancer-related deaths in men and women with a 5-year survival for all stages combined of only 16% [2]. The obvious need to develop better strategies for treating lung cancer should include improved detection methods and chemotherapeutics targeting lung cancer at early stages. Smoking is by far the most important risk factor for lung cancer [2]. Effective intervention in smokers and ex-smokers at initial stages of lung cancer could significantly impact the dismal prognosis of this deadly disease.

Epidermal growth factor receptor (EGFR) is expressed in a wide range of tumors of epithelial origin including non-small cell lung cancer (NSCLC) [3, 4], and is associated with a poor prognosis [5]. EGFR (also known as ErbB1 or HER-1) is one of four members of the ErbB receptor tyrosine kinase (TK) family that also includes ErbB2/HER2, ErbB3/HER3 and ErbB4/HER4 [6, 7]. Upon ligand binding by EGF or related growth factors to the extracellular domain of EGFR, receptor homo-dimerization or hetero-dimerization activates its intrinsic kinase activity. The resulting autophosphorylation of specific tyrosine residues within the intracellular domain of EGFR initiates a cascade of downstream signaling important for augmenting proliferation, decreasing apoptosis, and enhancing tumor cell motility [6, 7]. Aberrant EGFR signaling in cancer cells can consequently accelerate tumor progression, and much effort has focused on the development of a class of drugs that inhibits EGFR TK activity [8–10]. Erlotinib (Tarceva, OSI-774; OSI Pharmaceuticals, Roche, Genentech) and gefitinib (Iressa; Astra-Zeneca) are the two most extensively evaluated EGFR TK inhibitors (TKIs) in clinical trials [11, 12]. Erlotinib, a low molecular weight, orally available inhibitor that acts at the ATP-binding site of the TK domain, significantly improved survival of advanced NSCLC patients who failed standard chemotherapy in the pivotal Phase III BR.21 placebo-controlled study, and was consequently approved by the FDA for treating advanced NSCLC as a monotherapy [13].

Only a small percentage of patients treated with erlotinib or gefitinib exhibit responses, predominantly non-smokers, women, East Asians, and patients with adenocarcinomas (AC) displaying bronchioloalveolar features [13, 14]. Molecular predictors in lung tumors of responsiveness include *EGFR* mutations [15–17], absence of activating *Kras* mutations [18, 19], and amplification of the *EGFR* gene [20, 21]. Dozens of gain-of-function somatic EGFR mutations in exons 18–21 cluster around the TK domain of EGFR [15, 16, 22]. In NSCLC patients, these mutations occur more frequently in non-smokers, women, Asians and AC, providing a mechanistic basis of positive response in these subgroups. Yet, further analysis indicates that patients with mutant EGFR respond better to many therapeutics and some patients with wild-type EGFR respond to erlotinib therapy [13, 21, 23]. The effect of *Kras* mutations on EGFR TKI efficacy is unclear. Several reports indicate that *Kras* mutations confer resistance to erlotinib and gefitinib in NSCLC [18, 19], but lung tumors bearing *Kras* mutations are often present in smokers [24] and tend to be very aggressive with shortened survival irrespective of treatment [25]. In pancreatic cancer, a tumor-type where *Kras* mutations predominate, erlotinib increased overall survival in combination with gemcitabine chemotherapy in a Phase III study and was approved by the FDA for treatment of non-resectable pancreatic cancer [26]. Thus, the role of *EGFR* and *Kras* mutations in erlotinib efficacy is not completely understood and merits further investigation.

The low toxicity profile of EGFR TKIs compared with conventional chemotherapy make them attractive candidates for chemoprevention or early chemotherapy. Erlotinib is likely to be effective at earlier stages of lung cancer since increased EGFR expression is one of the first and most consistent abnormalities in the bronchial epithelium of smokers and EGFR expression is detected in initial lung cancer proliferative lesions [27, 28]. Given the success of erlotinib in advanced NSCLC treatment, the efficacy of erlotinib as an early chemotherapeutic merits investigation.

Carcinogen (urethane)-induced primary lung tumors in A/J mice provide an excellent model [29–31] for determining the efficacy of erlotinib as an early chemotherapeutic as well as evaluating mechanisms responsible for positive erlotinib activity. This experimental system can be vigorously examined throughout lung carcinogenesis, from the appearance of early pre-neoplastic proliferative lesions and small adenomas [32] to malignancy [33]. A/J and other stains of mice develop AC in response to chemical carcinogens, and AC comprises the majority of human NSCLC diagnoses. Primary mouse lung tumors share morphological, histogenic and molecular characteristics with human AC [30], including altered expression of common sets of genes as determined by global genomic analysis [33, 34], making it more analogous to human disease than tumor xenograft models. Chemical carcinogenesis more closely recapitulates the field carcinogenesis induced in humans by tobacco than recently developed congenic mouse lung tumor models that employ targeted expression of a single mutant gene, *Kras* [35, 36].

We evaluated erlotinib as a chemotherapeutic agent in small adenomas of male and female A/J mice exposed to urethane. These early lesions grew faster in male than in female mice, and erlotinib effectively reduced the size of adenomas in males but not females after a relatively brief administration period of 25 days. While no gender differences were observed in erlotinib pharmacokinetics (PK), levels of OSI-420, a metabolite of erlotinib with equivalent

activity against EGFR TK phosphorylation in vitro [37], were higher in tissues derived from males compared to females. Control males exhibited substantially higher levels of phosphorylated EGFR (pEGFR) relative to control females in both lung tumors and UI lung tissue, and erlotinib treatment inhibited EGFR phosphorylation in these tissues to a greater extent in males compared to females. Combined, these data suggest an increased dependence for EGFR-mediated signaling in small tumors growing in male mice compared to females that is susceptible to molecular targeting.

Materials and methods

Mice and erlotinib

Female and male A/J mice (7–10 weeks old) were purchased from Jackson Laboratories (Bar Harbor, ME) and maintained on hardwood bedding with a 12-h light/dark cycle, and given Teklad-8640 standard laboratory chow (Harlan Teklad, Madison, WI) and water ad libitum. A 10 mg/ml suspension of erlotinib® in 6% Captisol® vehicle, provided by OSI Pharmaceuticals (Melville, NY) and Cydex (Lenexa, KS) was diluted in sterile water or 6% Captisol for IP administration to mice (total injection volume was 0.16–0.32 ml using a tuberculin syringe).

Erlotinib studies in naïve mice

A/J mice (8 weeks old) were treated with 3, 10, 30 and 100 mg/kg body weight erlotinib daily for 5 days by IP administration, and weighed daily ($n = 5$ per treatment group). Twenty-four hours after the last erlotinib administration, mice were killed by lethal injection of 9 mg sodium pentobarbital with 100 U heparin (Sigma-Aldrich, St Louis, MO) in 0.9% NaCl. Blood samples were obtained by open cavity heart-puncture and centrifuged at low speed for 5 min at 24°C. The top plasma layer was transferred to a separate tube and stored at −80°C. Lung and liver samples were dissected, transferred to cryotubes, and stored in liquid nitrogen.

Erlotinib studies in tumor-bearing mice

Mice (7–10 weeks old) were treated with a single IP injection of the carcinogen, urethane, at 1 mg/g body weight (Sigma-Aldrich) dissolved in 0.9% NaCl, as previously described [38]. Sixteen weeks after urethane injection when small adenomas are well established, mice were treated with erlotinib. For the erlotinib half-life study, mice received a single IP injection of 10 mg/kg body weight erlotinib or 6% Captisol vehicle and were killed 0.5, 1, 4, 8 and 12 h later ($n = 2$ per timepoint). For the erlotinib therapeutic efficacy study, mice received daily IP injections of 10 mg/kg erlotinib or 6% Captisol vehicle on a 5-day on, 2-day off schedule for 3.5 weeks, totaling 18–20 total injections ($n = 14$–15 per treatment group). One hour after the last drug administration, animals were killed and plasma and liver harvested as described above. Lungs were removed and tumors were counted and dissected from adjacent uninvolved (UI) lung. Tumors from each mouse were pooled together, transferred to pre-tared cryotubes, and weighed to estimate total tumor burden. Tumor enumeration and weighing were conducted in a blinded fashion. Tumors and adjacent lung samples were stored immediately in liquid nitrogen.

Erlotinib and OSI 420/413 levels in mouse tissues

Erlotinib and the OSI-420/413 (OSI-420) metabolite levels, were measured in plasma, lung, lung tumors and liver samples by a validated isocratic reverse-phase high-performance liquid chromatography/tandem mass spectrometry method, as previously described [37, 39, 40]. Briefly, plasma or tissue homogenized in sodium phosphate buffered saline was combined with internal standard and absorbed to a diatomaceous earth cartridge. Liquid/liquid extraction with methyl tertiary butyl ether separated the analytes from plasma and tissue components. Following drying and resuspension, the retained analytes were separated with a Waters Symmetry C-18 column using ammonium formate buffer and methanol as the mobile phase. Erlotinib, OSI-420, and an internal standard were eluted from the column, ionized by heated nebulizer, and the mass transitions monitored at 394.4/278.0, 380.3/278.0, and 408.4/292.0 *m/z*, respectively.

EGFR and *Kras* mutation analyses

DNA was isolated from A/J mouse lung tumor tissue using the DNeasy® Tissue kit (Qiagen; Hilden, Germany and Nexttec; Germany). Exon specific primers used to PCR-amplify *Kras* exon 2, codon 61 were F-GGTCTTCTATTG TTGAGCTG and R-ACAGGAATTCTGCATACTTG. Exon specific primers for *EGFR* exons 18, 19, 20 and 21 were; 18F-CCACTGCTCCTTTGAACACA, 18R-CACT GGTTCCCAGAAGCCTA, 19F-CCCAGCACTCTTGGA TTTGT, 19R-CCCACGTCCCTATAAGCAGA, 20F-AA AGGGATATGCGTGCCTCT, 20R-CGTGGAAGACCA C AAGTCAA, 21F-CCGCATCAAGCAAAGTACAA and 21R-TTTGGCCTCTGAACAGGTCT. Each PCR reaction contained 10–100 ng DNA, 1X iQ™ Supermix (BioRad; Hercules, CA) and 150–175 ng forward and reverse primers in 50 µl. For *Kras*, the PCR cycling parameters were: 1 cycle of 95°C for 5 min, 25 cycles of 94°C for 30 s, 55°C for 30 s and 65°C for 30 s, and finally 1 cycle of 65°C for 5 min. For each *EGFR* exon, touchdown PCR

cycling parameters consisted of 4 steps: (1) 1 cycle of 94°C for 3 min, (2) 20 cycles of 94°C for 30 s, 65°C for 1 min (decreasing 0.5°C per cycle, ending at 55.5°C on cycle 20) and 72°C for 2 min, (3) 15 cycles of 94°C for 30 s, 55°C for 1 min and 72°C for 2 min, and (4) 1 cycle of 72°C for 5 min. The resulting PCR products were electrophoresed on a 2% agarose gel; a ladder of mass standards was used to estimate concentration and purity. A 15 ng aliquot was treated with ExoSAP-IT® (USB Corp.; Cleveland, OH) to remove unconsumed dNTPs and primers, and sequenced in the sense direction (*Kras*) or both sense and anti-sense directions (*EGFR*) by the UCDHSC Cancer Center Sequencing Core or by Northwoods DNA (Solway, MN).

Immunohistochemistry

Eight mice were killed and their lungs gently inflated through a canulated trachea with formalin for 1 h. Lungs were removed from the chest cavity and individual lobes separated and submerged in formalin overnight, and embedded in paraffin. Four μm sections were cut, deparaffinized, and endogenous peroxidase activity blocked with 1% hydrogen peroxide in methanol. Slides were submerged in 1 mM EDTA (Sigma-Aldrich) and microwaved for two 5 min cycles at full power interrupted by a 5 min pause to retrieve antigen before blocking with 10% goat serum (Sigma-Aldrich) and 20% avidin blocking solution (Vector Laboratories, Burlington, CA) in TNS (15 mM Tris, pH = 7.4, 150 mM NaCl). Slides were incubated with primary antibodies against EGFR (Cell Signaling Technology, Danvers, MA), diluted 1:50, or with phospho-EGFR(pTyr^{1068}; Zymed, South San Francisco, CA), diluted 1:1,300, with 20% biotin blocking solution (Vector Laboratories) and 10% goat serum in TNS for 2 h or 90 min, respectively, at 30°C in a humidified chamber. Addition of a biotinylated goat anti-rabbit secondary (1:200; Vector Laboratories) was followed by ABC complex incubation (Vector Laboratories). Immunostaining was achieved using the chromagen, diaminobenzidine (Sigma-Aldrich), with hematoxylin as the counter-stain.

Immunoblotting

Dissected lung tumors and adjacent UI lungs were submerged in 4°C 200–800 μl cell extraction buffer (Biosource, Camarillo, CA) with Mini Complete®, protease inhibitor cocktail (Roche Applied Science, Indianapolis, IN). Samples were Dounce-homogenized on ice, incubated for 30 min at 4°C, sonicated, centrifuged at 16,000×*g* for 10 min, and supernatants retained and stored at −80°C. An aliquot of each sample was assessed for protein concentration by the method of Lowry et al. [41], and the remainder mixed with a 1:1 dilution of 2× gel-loading buffer (100 mM Tris pH 6.8, 0.4% sodium dodecyl sulfate, 2% β-mercaptoethanol, 20% glycerol and 0.3% pyronine Y) and incubated at 100°C for 5 min. Equal amounts of proteins (100–150 μg) were resolved on a 6% SDS-polyacrylamide gel followed by transfer on to an Immobilon-P PVDF membrane (Millipore Corp., Bedford, MA) and blocked in 5% non-fat dried milk with 0.1% Tween 20 in TNS for 30 min. Membranes were incubated with primary antibodies against EGFR at a 1:100 dilution overnight, or phospho-specific EGFR (pTyr^{1068}) at 0.1 μg/ml with 0.1%Tween 20 in TNS for 1 h at 4°C followed by wash buffer (2% milk, 0.1% Tween 20 in TNS). Addition of goat anti-rabbit secondary (Santa Cruz Biotechnology, Santa Cruz, CA) at 0.02 μg/ml with 0.1%Tween 20 in TNS for 1 h was followed by wash buffer. Protein bands were visualized by incubation with Western Lighting (PE Applied Biosystems, Foster, CA) or Supersignal (Pierce, Rockford, IL) chemiluminescent substrate, exposed to CL-Xposure X-ray film (Pierce), and bands were quantified by Un-Scan-It software (Silk Scientific, Orem, UT). Equal protein loading was confirmed by Ponceau-staining of membranes in addition to pan-EGFR immunoblots.

Statistical analysis

Data are represented as mean ± SEM, and analyzed by Student's unpaired *t*-test with Prism 3.0 software (Graphpad, San Diego, CA), except *Kras* mutation incidence which was evaluated by Yates-corrected chi-square test. In all analyses, significance of $p \leq 0.05$ was accepted.

Results

Assessment of erlotinib toxicity and bioavailability in A/J mice

A dose-response study was conducted to determine the erlotinib concentration range that can be administered without toxicity as well as drug bioavailability. Eight-week-old male and female A/J mice were treated with 3, 10, 30 and 100 mg/kg body weight erlotinib daily for 5 days by IP administration (five mice per treatment group). To assess toxicity, animals were weighed 24 h after each erlotinib injection (Fig. 1). The 100 mg/kg dose caused 9 and 12% weight loss in female and male mice, respectively, with the greatest weight loss occurring within the first 24 h. The 30 mg/kg elicited a notable 5–6% weight loss. As these toxicities were observed after only a 5-day treatment, the 30 and 100 mg/kg doses were not used in subsequent long-term studies. The 3 and 10 mg/kg doses resulted in minimal weight loss in both male and female animals (no more then 3%). No alopecia or skin problems were obvious at any dose.

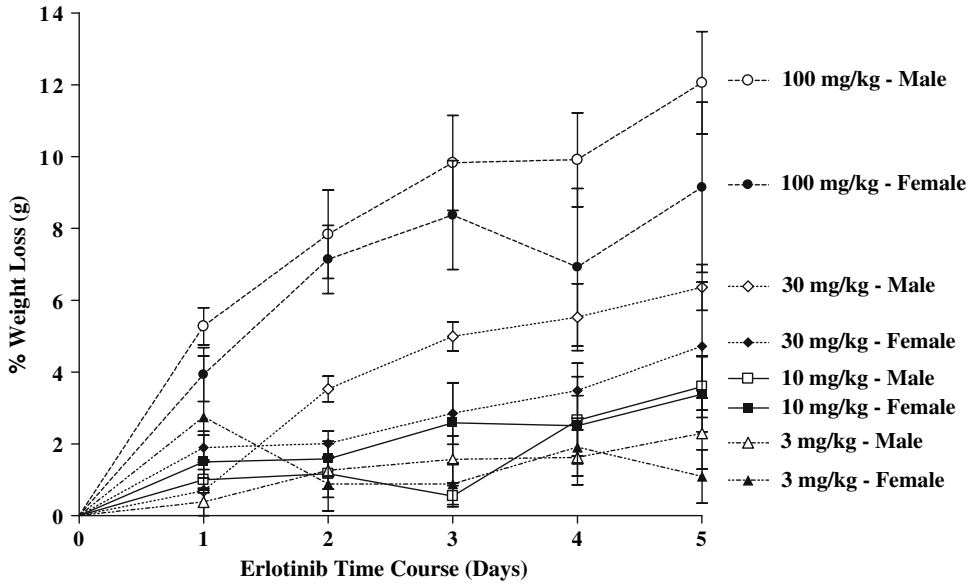

Fig. 1 Effect of erlotinib on weight loss in A/J mice. Female and male A/J mice were treated with 3, 10, 30 or 100 mg/kg body weight erlotinib daily for 5 days by IP administration ($n = 5$ per treatment group), and weighed 24 h after each drug administration

Erlotinib levels were measured in plasma and liver tissue, the primary site of erlotinib metabolism, 24 h after the last erlotinib IP injection, as described in "Materials and methods" section (Fig. 2). OSI-420 and OSI-413 were also assayed as they are the most prominent circulating metabolites of erlotinib [42] and have in vitro cellular activities against EGFR similar to erlotinib (data on file at OSI Pharmaceuticals). The bioanalytical method used to measure OSI-420 and OSI-413 does not distinguish between them as they result from *O*-demethylation of either side chain in the primary compound, so they were quantified together and are collectively referred to as OSI-420 [37] as shown in Fig. 2b, d. Plasma levels of erlotinib increased in a dose-dependent manner and were similar in male and female mice at the 10, 30 and 100 mg/kg doses (Fig. 2a), indicating that erlotinib is bioavailable in both genders of A/J mice. The amount of OSI-420 in plasma generally increased with dose with levels higher in male versus female samples at the 10 and 100 mg/kg doses, however this trend was not significant (Fig. 2b). At the 3 mg/kg dose, neither erlotinib nor OSI-420 levels were above the limits of detection (1 ng/ml). In vitro studies in human cells indicate that erlotinib is mainly metabolized by hepatic enzymes, CYP1A2 and CYP3A4 [42]. Hepatic levels of erlotinib and OSI-420 increased dose-dependently in male and female mice (Fig. 2c, d). In mice receiving the 100 mg/kg dose, erlotinib accumulated up to 25,000 ng/g tissue weight; however, these livers exhibited abnormal white spots upon gross examination and a fatty liver phenotype by histological analysis. These pathologies, along with the weight loss described above, confirmed toxicity at the 100 mg/kg dose. Extrahepatic metabolism may be mediated by CYP3A4 in the intestine, CYP1A1 in the lungs, and CYP1B1 in tumor tissue [42]. Erlotinib and OSI-420 were assayed in lung tissue but detected only at the 100 mg/kg dose (data not shown).

Erlotinib and OSI-420 half-lives in tumor-bearing mice

To determine levels of erlotinib and OSI-420 at earlier timepoints after drug administration and establish if biologically relevant levels accumulate in lung tumors (0.1–2 μM) [43, 44], a half-life study was conducted in tumor-bearing animals. A/J mice were injected with 1 mg/g body weight of the carcinogen, urethane, and tumors allowed to develop for 16 weeks, a timepoint when multiple, small, lung nodules (adenomas) composed of uniform-looking cells (~40 tumors per mouse, 500–800 μm diameter) can be observed [32]. Adenocarcinoma with increased disorganization of tumor cells and invasion into the stroma is typically not observed in this model until 30 weeks after urethane treatment [33]. After 16 weeks, mice received a single IP injection of 10 mg/kg erlotinib, and they were killed 0.5, 1, 4, 8 or 12 h later. Plasma, lung tumors, adjacent UI lung tissue (i.e., pulmonary tissue in tumor-bearing mice with no grossly observable lesions), and liver were immediately harvested and analyzed as described in "Materials and methods" section.

The elimination pattern of both erlotinib and OSI-420 was comparable between genders in all tissues assessed (Fig. 3). Plasma erlotinib levels were highest at 0.5 h in male and female mice at 4,500 and 5,500 ng/ml, respectively, and the half-lives were 1.8 and 1.4 h, respectively. Erlotinib half-lives were not significantly different between males and females in lung tumors ($T_{1/2} = 1.2$ and 1.4 h, respectively), UI lung ($T_{1/2} = 1.5$ and 1.6 h, respectively), and liver samples ($T_{1/2} = 0.9$ and 2.0 h, respectively) as shown in Fig. 3c, e, g, respectively. OSI-420 levels were

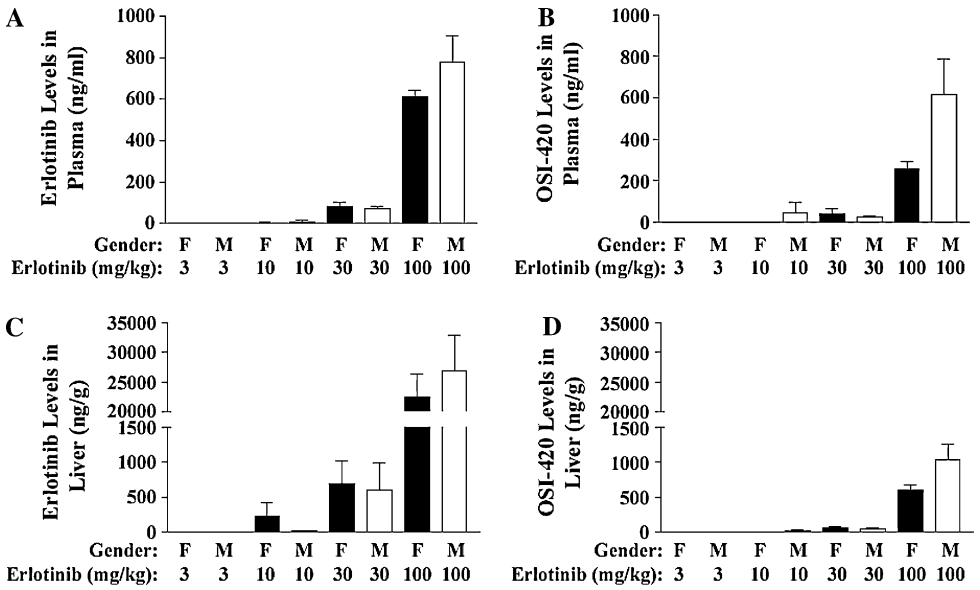

Fig. 2 Erlotinib (**a**) and OSI-420 (**b**) levels in plasma and erlotinib (**c**) and OSI-420 (**d**) levels in liver. Female and male A/J mice were treated with 3, 10, 30 or 100 mg/kg body weight erlotinib daily for 5 days by IP administration ($n = 5$ per treatment group). Plasma and liver tissue was harvested from each mouse 24 h after the last erlotinib administration, and assayed for erlotinib and OSI-420 concentration by reverse-phase HPLC/tandem mass spectrometry as described in "Materials and methods" section. In mice treated with 3 mg/kg erlotinib, the levels of erlotinib and OSI-420 levels were below the limit of detection (1 ng/ml) in all tissues. Neither erlotinib nor OSI-420 levels were statistically different between genders in all tissues assessed

10–15% of erlotinib levels, with half-lives ranging from 2.2 to 3.8 h in all tissues evaluated from males and females (Fig. 3b, d, f, h). Substantial amounts of erlotinib and OSI-420 were observed in liver (3,500–6,000 and 300–500 ng/ml peak levels, respectively), consistent with the hepatic metabolism of these compounds (Fig. 3g, h, respectively). Interestingly, erlotinib levels were 2.5-fold higher in tumors relative to adjacent UI lungs in both males (3,605 and 1,330 ng/ml average peak levels, respectively) and females (3,595 and 1,495 ng/ml average peak levels, respectively). OSI-420 levels concentrated in tumors to an even greater extent (five- to sixfold increases) in both genders. The IC_{50} of erlotinib for in vitro growth inhibition in sensitive human NSCLC cell lines ranges from 0.1 to 2 μM or 42 to 840 ng/ml [43, 44]. Therefore, erlotinib levels in mouse plasma, which ranged from ~200 to 5,000 ng/ml (0.5–12 μM) up to 8 h after drug administration, were either within the concentration range required to impact sensitive cells or at substantially greater concentrations. More importantly with regard to therapeutics, biologically relevant levels of erlotinib were achieved in lung tumors, ranging from 3,500 ng/g or ng/cm^3 (8 μM) at peak levels to averages over 700 ng/g (2 μM) up to 4 h after erlotinib administration.

Erlotinib efficacy as an early chemotherapeutic agent

The anti-cancer activity of erlotinib against urethane-induced lung tumors in A/J mice was determined. The 10 mg/kg erlotinib dose was chosen for this experiment because this dose: (1) is analogous to the 150 mg erlotinib per day dose administered to lung cancer patients (2 mg/kg in a 75 kg individual) [13]; (2) elicited minimal toxicity in A/J mice (<3% mouse weight loss, Fig. 1); and (3) resulted in biologically relevant levels of erlotinib in plasma and lung tumors in tumor-bearing A/J mice (Fig. 3).

Male and female A/J mice bearing early-stage lung cancer were treated with 10 mg/kg erlotinib or Captisol vehicle for 3.5 weeks as described in "Materials and methods" section. Mice exhibited no more than 5% (erlotinib) or 3% (vehicle) weight losses by the end of the study. One hour after the final drug administration, animals were killed and the tumor numbers and pooled weights of all tumors from an individual mouse determined as described in "Materials and methods" section. No differences in tumor multiplicity were observed between erlotinib-treated and Captisol-treated male or female mice (Fig. 4). Males had more tumors then females in both treatment groups; 39.7 ± 2.2 vs 35.6 ± 1.7, respectively, with Captisol and 39.9 ± 2.1 vs 37.5 ± 1.8, respectively, with erlotinib, but these differences were not significant.

Figure 5 demonstrates two interesting findings. First, tumors in male mice receiving vehicle alone grew significantly faster than tumors in vehicle-treated female mice, (total tumor weights = 26.2 ± 2.5 vs 11.9 ± 0.9 mg, respectively; $p < 0.0001$). Urethane-induced lung tumors also grow faster in males than in females in other studies carried out in our laboratory. Secondly, these fast-growing

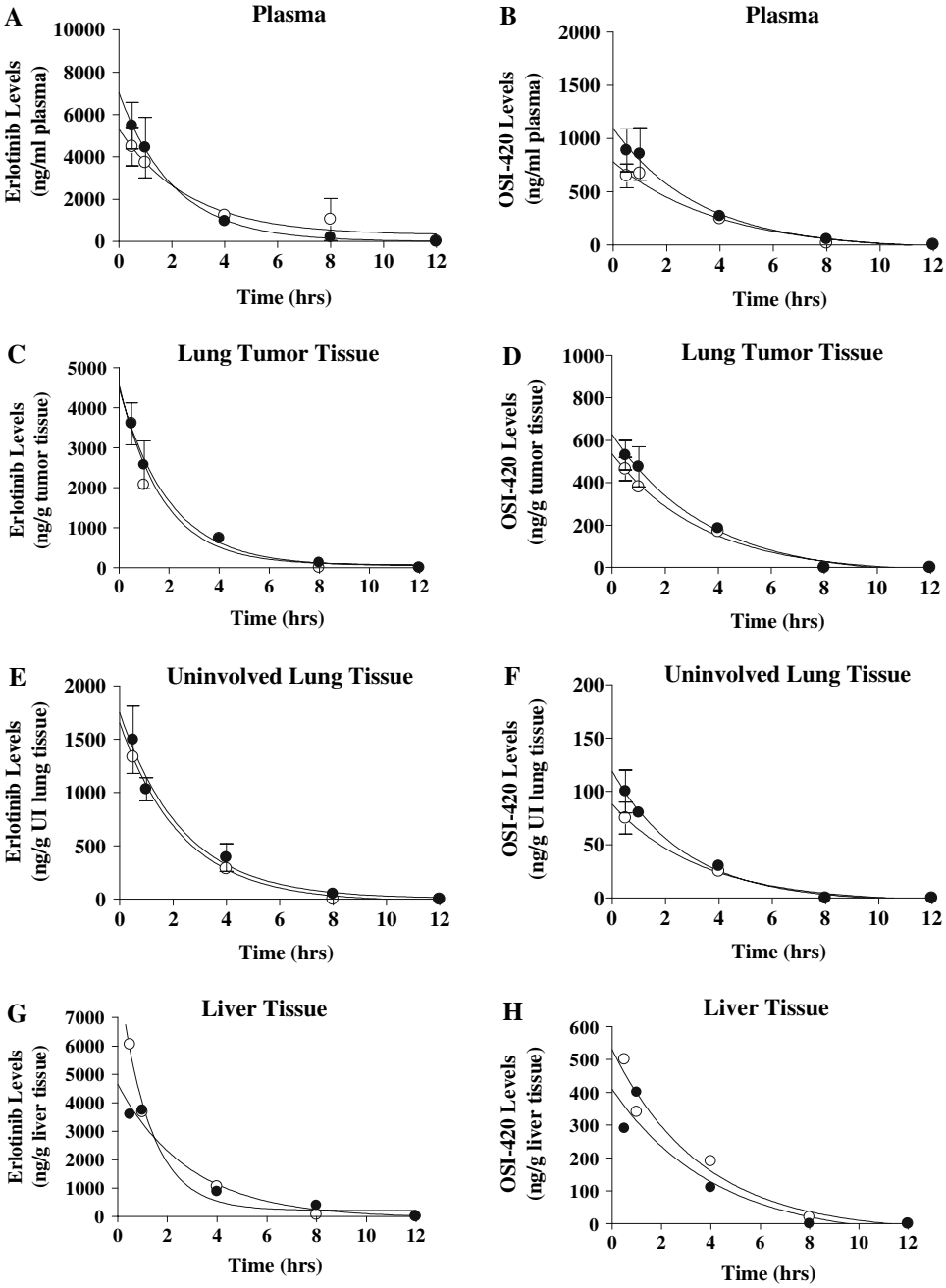

Fig. 3 Erlotinib and OSI-420 half-lives in tumor-bearing mice. Female (*filled circle*) and male (*open circle*) A/J mice were injected once with 1 mg/g body weight urethane to induce lung tumors. After 16 weeks, mice were treated with a single IP injection of 10 mg/kg erlotinib, killed after 0.5, 1, 4, 8 or 12 h at which time tissues were immediately harvested ($n = 2$ per timepoint; except liver where $n = 1$). Erlotinib levels were measured in plasma (**a**), lung tumor tissue (**c**), UI lung tissue (**e**) and liver tissue (**g**) and OSI-420 levels were measured in plasma (**b**), lung tumor tissue (**d**), UI lung tissue (**f**) and liver tissue (**h**) by reverse-phase HPLC/tandem mass spectrometry as described in "Materials and methods" section. *Plots* were evaluated by non-linear regression and one phase exponential decay using Graphpad Prism 3.0 software

lung tumors in male mice were over twofold smaller after the 3.5-week period of erlotinib treatment (12.7 ± 1.2 mg in the erlotinib group vs 26.2 ± 2.5 mg in the Captisol group; $p < 0.0001$). In contrast, the tumor burden in female mice increased with erlotinib by 21% (15.1 ± 1.2 in the erlotinib group vs 11.9 ± 0.9 in the Captisol group; $p < 0.05$). These data clearly show that erlotinib has promising activity at early stages of lung cancer in males after a relatively short 3.5-week treatment. Male dependent erlotinib-induced tumor shrinkage may result from gender differences in erlotinib metabolism and/or tumor biology, as discussed below.

Erlotinib and OSI-420 levels in the therapeutic efficacy study

To determine if differential metabolism of erlotinib and/or formation of OSI-420 could account for the gender-dependent inhibition of tumor growth by erlotinib, levels of the parent drug and metabolites were assessed in plasma, lung tumors and adjacent UI lung samples from the efficacy study described above (measured 1 h after the last drug administration). No significant differences in erlotinib levels were observed between male and female mice in plasma, 2,189 ± 135 and 2,106 ± 85 ng/ml, respectively;

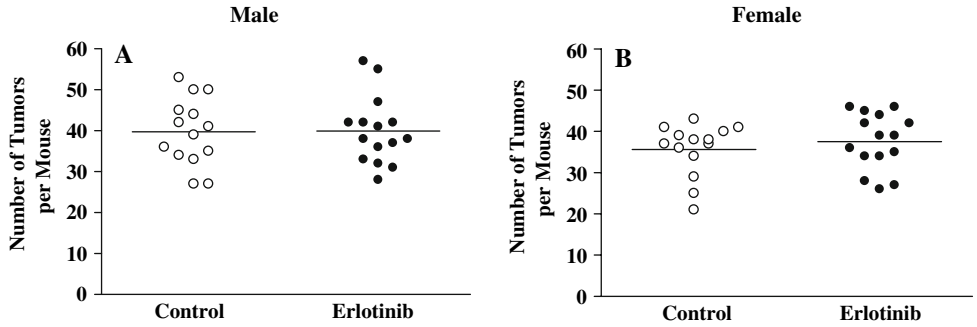

Fig. 4 Effect of erlotinib on lung tumor-number. Male (**a**) and female (**b**) A/J mice were injected once with 1 mg/g body weight urethane to induce lung tumors. After 16 weeks, mice received daily IP injections of 10 mg/kg erlotinib or 6% Captisol vehicle control on a 5-day on, 2-day off schedule for 3.5 weeks (18–20 total injections) and were killed 1 h after the last drug administration (14–15 mice per group). Lungs were removed, tumors dissected from adjacent UI lung, and counted in a blinded fashion. In both males and females, there was no significant difference in tumor number between control vehicle- and erlotinib-treated animals

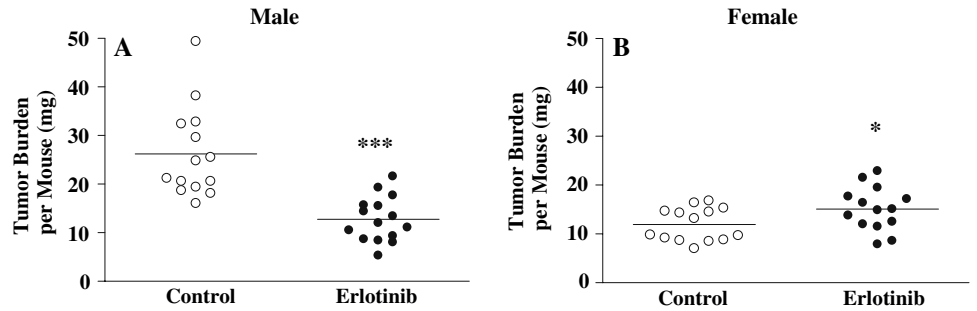

Fig. 5 Effect of erlotinib on lung tumor-burden. Male (**a**) and female (**b**) A/J mice were injected once with 1 mg/g body weight urethane to induce lung tumors. After 16 weeks, mice received daily IP injections of 10 mg/kg erlotinib or 6% Captisol vehicle control on a 5-day on, 2-day off schedule for 3.5 weeks (18–20 total injections) and were killed 1 h after the last drug administration (14–15 mice per group). Lungs were removed, tumors dissected from adjacent UI lung, and the pooled weights of all tumors from each individual mouse measured in a blinded fashion to determine total tumor burden. Male control vs male erlotinib, $p < 0.0001$; female control vs female erlotinib, $p < 0.05$ and male control vs female control, $p < 0.0001$

tumor tissue, 2,150 ± 253 and 1,750 ± 232 ng/g, respectively or adjacent UI lung, 1,100 ± 280 and 975 ± 103 ng/g, respectively (Fig. 6a–c, respectively). Therefore, differences in erlotinib accumulation cannot account for the greater sensitivity of male lung tumors to erlotinib. Amounts of erlotinib in all samples were well above the concentrations needed to impact sensitive cell lines (42–840 ng/ml or 0.1–2 μM; [43, 44]).

Significant gender differences in OSI-420 levels were noted, however. Male mice accumulated 50% more OSI-420 than female mice in plasma (597 ± 22 vs 403 ± 14 ng/ml, respectively, $p < 0.0001$) and also contained more of this metabolite in adjacent UI lungs (133 ± 15 vs 88 ± 9 ng/g, respectively, $p < 0.05$), as shown in Fig. 6d, f, respectively. The amount of OSI-420 in lung tumors from male mice was nearly twice that in females (643 ± 63 vs 355 ± 22 ng/g, respectively, $p = 0.005$; Fig. 6e). This is in contrast to the half-life study shown above (Fig. 3) where OSI-420 levels were similar between males and females in all tissues assessed over 24 h following a single erlotinib administration. Combined, these data imply that gender differences in OSI-420 accumulation depend upon whether erlotinib is administered as a single dose or as multiple doses over a 3.5-week timecourse. With chronic treatment, females either catabolize OSI-420 more rapidly than males or males convert more erlotinib to this metabolite than females.

Molecular determinants of erlotinib efficacy: *Kras* and *EGFR* mutations

Activating codon 12 mutations in the oncogene, *Kras*, negatively correlates with response of lung cancer patients to gefitinib and erlotinib [18, 19]. We assessed whether *Kras* mutation varied in tumors derived from male or female mice in the erlotinib efficacy study. Because urethane induces *Kras* mutations at codon 61 [45, 46], this amino acid was sequenced in all tumors (ca. 40 tumors per mouse) from four male and four female tumor-bearing mice, half of which received Captisol control and the other half erlotinib (~320 tumors altogether). In human lung AC, activating *Kras* mutations predominately occur at codon 12, however

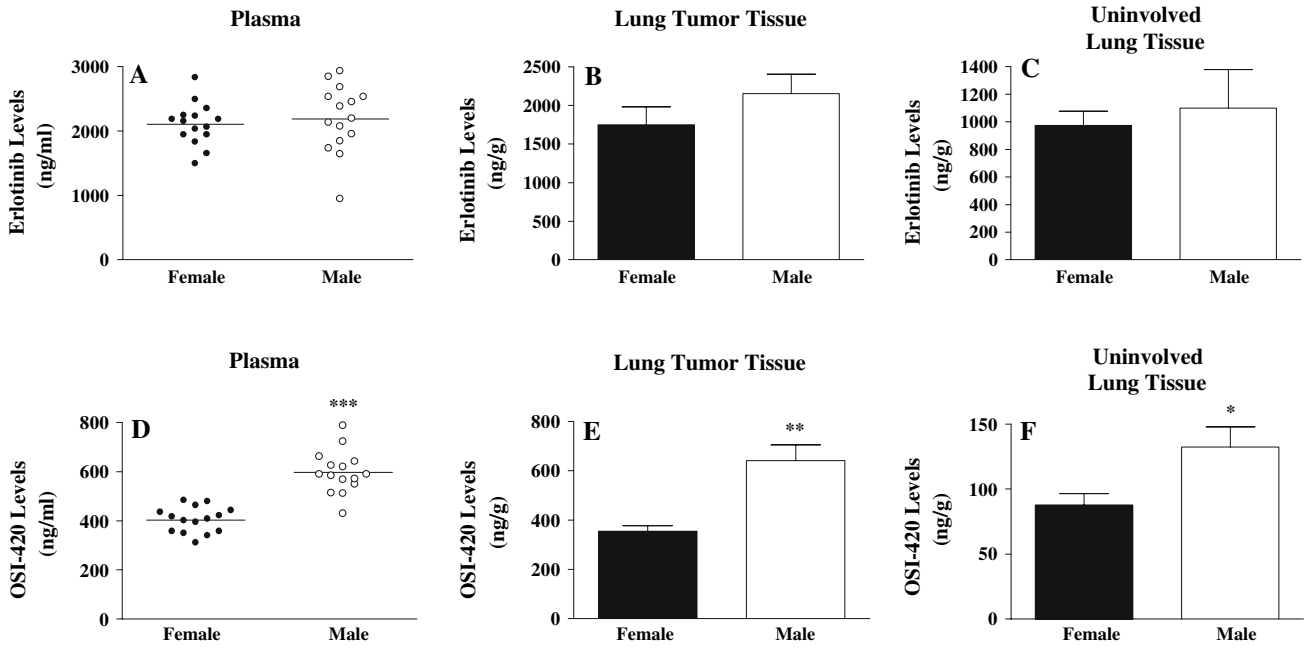

Fig. 6 Erlotinib levels in plasma (**a**), lung tumor tissue (**b**) and UI lung tissue (**c**) and OSI-420 levels in plasma (**d**), lung tumor tissue (**e**) and UI lung tissue (**f**). Female (*black*) and male (*white*) A/J mice were injected once with 1 mg/g body weight urethane to induce lung tumors. After 16 weeks, mice received daily IP injections of 10 mg/kg erlotinib or 6% Captisol vehicle control on a 5-day on, 2-day off schedule for 3.5 weeks (18–20 total injections). Mice were killed 1 h after the last drug administration and plasma (15 mice per group), lung tumor (4 mice per group) and adjacent normal appearing lung tissues (4 mice per group) were harvested. Erlotinib and OSI-420 levels were measured by reverse-phase HPLC/tandem mass spectrometry as described in "Materials and methods" section. Levels of erlotinib were not significantly different between genders in all tissues assessed. Levels of OSI-420 were significantly greater in males vs females in plasma, $p < 0.0001$; lung tumor tissue, $p = 0.005$ and uninvolved lung tissue, $p < 0.05$

mutations at codons 12 and 61 elicit similar inhibition of GTPase activity to constitutively activate *Kras* and downstream signaling [47]. There was no difference between male and female mice in the percentage of tumors bearing *Kras* mutations in animals treated with Captisol (77 and 81%, respectively), and these percentages were unchanged by erlotinib treatment (77 and 81%, respectively) as shown in Table 1. Interestingly, a gender difference in the type of *Kras* mutation was observed. Males had more Q61R mutations relative to females (26 and 11%, respectively) and fewer Q61L mutations (51 and 70%, respectively) in Captisol-treated animals (Table 1). Values were similar in erlotinib-treated mice. As *Kras* mutation incidence was not altered by erlotinib treatment in either gender, the Q61R and Q61L incidences for all male mice was compared against all female mice to reveal significant gender bias ($p \leq 0.05$ by chi-square test with Captisol- and erlotinib-treated animals grouped together by gender, Table 1). Importantly, these data combined with the efficacy data in Fig. 5 clearly show that tumors harboring *Kras* mutations in male mice shrink in response to erlotinib, indicating that *Kras* mutation and anti-EGFR TK activity against early pulmonary lesions are not mutually exclusive.

Some somatic tumor mutations in the ATP-binding region of the TK domain of *EGFR* correlate with favorable response to erlotinib and gefitinib in clinical trials [15, 16]. Over 40 mutations have been identified in *EGFR* exons 18–21, with nearly 90% as short, in-frame deletions in exon 19 that eliminate four amino acids (LREA) at positions 745–748 or point mutations at amino acid 858 (exon 21), resulting in the substitution of arginine for leucine (L858R) [22]. These four exons were sequenced in lung tumors from male and female mice to determine if the observed male-specific erlotinib response corresponds with any gender dependence of *EGFR* mutation incidence or type. Tumors were dissected from male and female A/J mice treated with 0, 3 or 10 mg/kg erlotinib daily for 6 days (four mice per treatment group), and DNA isolated from one tumor per mouse; altogether 24 randomly selected tumors were analyzed. The four *EGFR* exons were sequenced in both sense and anti-sense directions, as described in "Materials and methods" section. No *EGFR* mutations were detected in any tumor (Table 1), suggesting that *EGFR* mutation does not contribute to the positive response to erlotinib observed in male mice.

Cellular determinants of erlotinib efficacy: EGFR and phosphorylated EGFR localization and expression

Differential EGFR concentration and/or phosphorylation status between genders could also contribute to the male-specific

Table 1 *Kras* and *EGFR* mutations in male and female mouse lung tumors

Gene	Gender	Erlotinib dose (mg/kg)	Number of mice analyzed	Number of tumors analyzed per mouse	Exons analyzed	Mutation type
Kras	M	0	2	40, 32	2	Total, 77% Q61L, 51% Q61R, 26%
	M	10	2	41, 38	2	Total, 77% Q61L, 58% Q61R, 19%
	F	0	2	35, 28	2	Total, 81% Q61L, 70% Q61R, 11%
	F	10	2	37, 25	2	Total, 81% Q61L, 65% Q61R, 16%
EGFR	M	0	4	1	18, 19, 20, 21	None
	M	3	4	1	18, 19, 20, 21	None
	M	10	4	1	18, 19, 20, 21	None
	F	0	4	1	18, 19, 20, 21	None
	F	3	4	1	18, 19, 20, 21	None
	F	10	4	1	18, 19, 20, 21	None

efficacy of erlotinib. There were no apparent differences between males and females in the expression pattern of total EGFR in adjacent UI lung (Fig. 7a, b, respectively) or lung tumors treated with Captisol control (Fig. 7c, d, respectively), as analyzed by immunohistochemistry. Tumor immunostaining from Captisol-treated animals was similar to 10 mg/kg erlotinib-treated males (Fig. 7c, e, respectively) and females (Fig. 7d, f, respectively). In UI lung tissue, EGFR was most strongly expressed in Clara cells (Fig. 7a, b). Lighter staining was also observed in type I and type II cells and alveolar macrophages as identified by morphology and location. In lung tumors, EGFR was expressed in the majority of cells but with varying intensities (Fig. 7c–f). In positively stained cells, EGFR was completely absent from nuclei, as expected for a plasma membrane receptor.

Phosphorylation at tyrosine-1068 was evaluated because downstream signaling involved in survival (phosphatidylinositol 3-kinase (PI3K)-AKT and signal transducer and activator of transcription (STAT) pathways) appears to couple to EGFR activation at this site [9, 48]. Phospho-EGFR(Tyr^{1068})-immunostaining in Captisol-treated animals was stronger in male UI lungs than in female UI lung tissue (Fig. 7g, h, respectively). Immunostaining was darkest in Clara cells (Fig. 7g, h). Expression was also observed in type I and type II cells and macrophages as identified by morphology and location (depicted in Fig. 7g). Phospho-EGFR(Tyr^{1068}) staining was more pronounced in tumors from male Captisol-treated mice than females (Fig. 7i, j, respectively). This activated receptor protein localized at the edges of distinct circular acinar-like structures, consistent with localization on a polarized plasma membrane (Fig. 7i, j). After erlotinib treatment, this pattern disappeared and immunostaining was more diffuse throughout the tumor. Further, the intensity of phospho-EGFR(Tyr^{1068}) expression decreased to a much greater extent in tumors from male mice as compared to female mice (compare Fig. 7i, k vs j, l, respectively).

To confirm these immunohistochemistry results, total EGFR and phospho-EGFR(Tyr^{1068}) levels were quantified in lung tissues by immunoblotting. Total EGFR levels were similar between males and females in UI lungs and unaffected by erlotinib treatment (Fig. 8a). Consequently, total EGFR levels were used as a loading control for subsequent phospho-EGFR(Tyr^{1068}) immunoblots; (β-actin, the protein commonly used as an immunoblot loading control was not used as its expression was greater in male compared to female tumors and UI lung tissue). pEGFR levels, however, were 2.5-fold greater in UI lung derived from males compared to females (1.16 ± 0.14 and 0.47 ± 0.18 ratio of pEGFR/EGFR relative densitometric units, respectively, $p < 0.05$; Fig. 8a, b). Erlotinib treatment reduced the amount of phospho-EGFR(Tyr^{1068}) in UI tissue from males by 3.4-fold compared to controls (0.34 ± 0.08 and 1.16 ± 0.14 ratio of pEGFR/EGFR relative densitometric units, respectively, $p < 0.01$); a decrease was observed in females but was not statistically significant (Fig. 8b). In tumors, total EGFR levels were also similar between males and females and not affected by erlotinib treatment (Fig. 8c). Impressively, phospho-EGFR(Tyr^{1068}) detection was sevenfold higher in tumors from males compared to females (1.20 ± 0.15 and 0.17 ± 0.04 ratio of pEGFR/EGFR relative densitometric

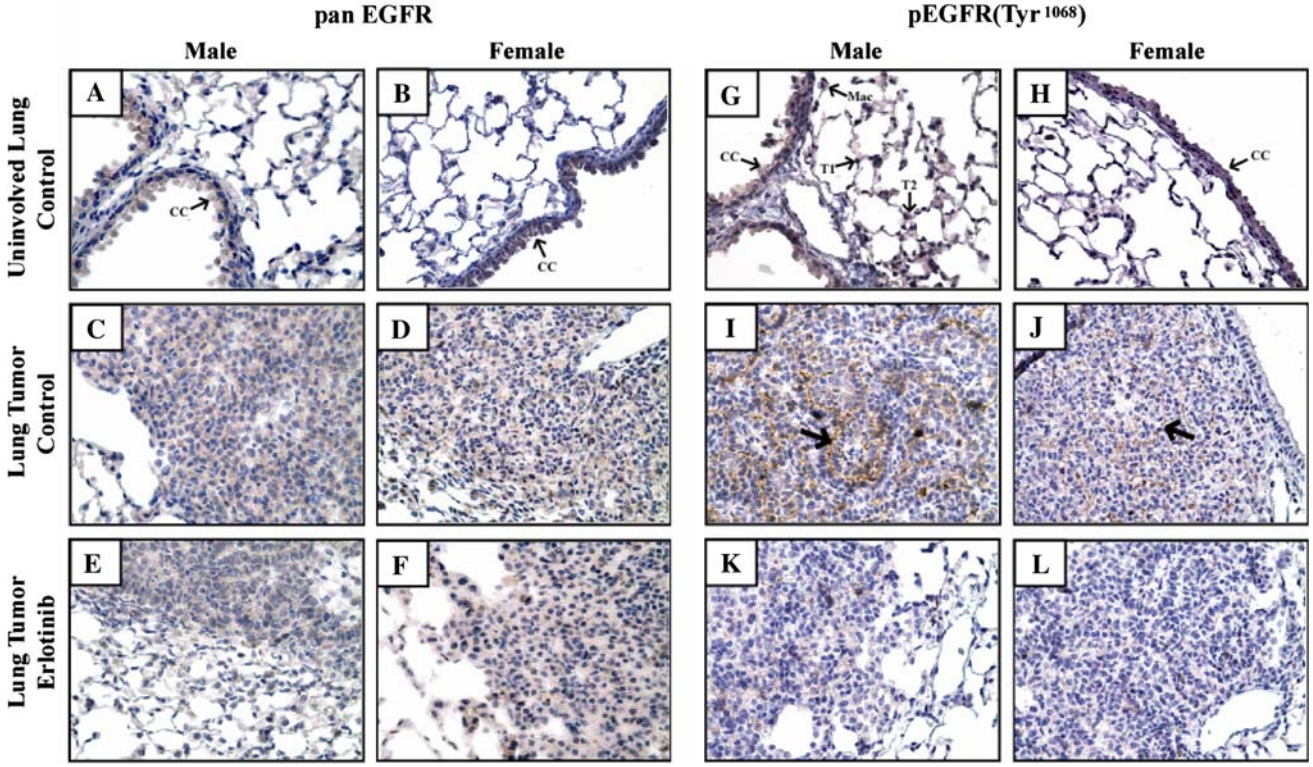

Fig. 7 Effect of erlotinib on total EGFR and phosphorylated EGFR localization in tumors from male and female mice. Immunohistochemistry of total EGFR in adjacent UI lung in a male (**a**) and female (**b**) mouse treated with Captisol vehicle, lung tumors from male mice treated with Captisol vehicle (**c**) or erlotinib (**e**) and lung tumors from female mice treated with Captisol vehicle (**d**) or erlotinib (**f**) and pEGFR(Tyr^{1068}) in adjacent UI lung in a male (**g**) and female (**h**) mouse treated with Captisol vehicle, lung tumors from male mice treated with Captisol vehicle (**i**) or erlotinib (**k**) and lung tumors from female mice treated with Captisol vehicle (**j**) or erlotinib (**l**). Samples were obtained from A/J mice injected once with 1 mg/g body weight urethane to induce lung tumors. After 16 weeks, mice received daily IP injections of 10 mg/kg erlotinib or 6% Captisol vehicle control for 3.5 weeks as described in "Materials and methods" section. One hour after the last drug administration, animals were killed, lungs removed, embedded in paraffin blocs and cut into 4 μm sections. Samples are representative of $n = 2$ for each treatment group. EGFR and pEGFR(Tyr^{1068}) positive cells are brown. Hematoxylin counterstain. *CC* Clara cell, *Mac* macrophage, *T1* Type I cell, *T2* Type II cell, → acinar structure. Original magnification ×400

units, respectively, $p < 0.005$; Fig. 8c, d). Most importantly, treatment with erlotinib decreased pEGFR levels in male tumors twofold compared to control animals (0.57 ± 0.12 and 1.20 ± 0.15 ratio of pEGFR/EGFR relative densitometric units, respectively, $p < 0.005$; Fig. 8d) but did not affect female levels (Fig. 8d).

These combined immunohistochemistry and immunoblotting results provide strong evidence that the ability of erlotinib to shrink lung tumors in male but not female mice is associated with selective inhibition of EGFR phosphorylation in males. This may result from a greater dependence of male tumor maintenance on the EGFR pathway, suggested by the higher levels of pEGFR in tumors from male mice compared to tumors from females.

Discussion

To date, erlotinib has primarily been tested in clinical trials of patients with end-stage metastatic lung cancer and is approved for advanced NSCLC as a monotherapy in patients who have failed standard chemotherapy [13]. Here we show that erlotinib was also effective as an early chemotherapeutic in a chemically induced mouse model of lung AC in male mice. After a 3.5-week administration period, erlotinib significantly decreased the total burden of small, early-stage adenomas in male mice twofold as compared to vehicle, while tumor burden in erlotinib-treated females increased by 21%. The basis of this gender discordance in efficacy could be due to sexual dimorphisms in PK factors, tumor biology, or both, as discussed below.

Gender differences in erlotinib PK

Neither the accumulation or half-life of erlotinib differed in plasma, lung tumors or adjacent UI lung between male and female mice treated with 10 mg/kg erlotinib, as shown in Figs. 6 and 3, respectively. There were significantly higher levels of the erlotinib metabolite, OSI-420, in males compared to females in all of these tissues when erlotinib was

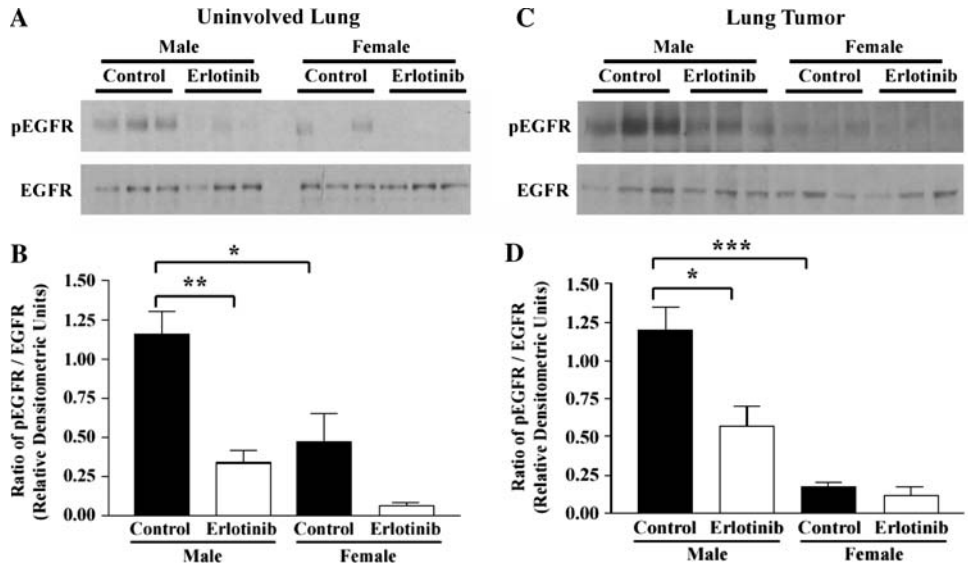

Fig. 8 Effect of erlotinib on pEGFR and total EGFR levels in adjacent UI lung tissue and lung tumors from male and female mice. Immunoblotting of phospho-EGFR(Tyr^{1068}) and total EGFR in UI lung tissue (**a**) and lung tumors (**c**). Samples were obtained from male and female A/J mice injected once with 1 mg/g body weight urethane to induce lung tumors. After 16 weeks, mice received daily IP injections of 10 mg/kg erlotinib or 6% Captisol vehicle control on a 5-day on, 2-day off schedule for 3.5 weeks. Mice were killed 1 h after the last drug administration and adjacent UI lung was dissected from tumors, processed and pEGFR(Tyr^{1068}) and EGFR levels detected by immunoblot analysis; $n = 3$. Because EGFR levels are similar in all samples, it is used as an internal control. Densitometric analysis represents mean ± SEM of the ratio of pEGFR/total EGFR in UI lung (**b**) and lung tumors (**d**); $n = 3$. In UI lung samples, male control vs male erlotinib, $p < 0.01$, male control vs female control, $p < 0.05$ and female control vs female erlotinib, $p = 0.0818$ (**b**) and in lung tumor samples, male control vs male erlotinib, $p < 0.05$, male control vs female control, $p < 0.005$ and female control vs female erlotinib, $p = 0.4613$ (**d**)

applied over 3.5 weeks (Fig. 6), but not when administered acutely as a single injection in the half-life study (Fig. 3). These results imply that when erlotinib is chronically administered to mice, females either catabolize OSI-420 more rapidly than males or males convert more erlotinib to OSI-420 than females. The latter hypothesis should result in lower levels of erlotinib in males compared to females, but this was not the case. Thus, more rapid catabolism of OSI-420 in females probably accounts for their lower OSI-420 levels. Enzymes responsible for OSI-420 catabolism or clearance may be more highly induced in females than males in mice exposed to erlotinib for several weeks. Gender differences in the pulmonary metabolism of xenobiotics have been noted previously in mice, with the nature of this dimorphism being drug-specific. Male mice metabolize styrene more extensively than females, whereas females metabolize 1–1-dichloroethylene and napththalene to a greater extent than males [49]. Erlotinib levels in plasma and lung tumors were also affected by short or long-term exposure to erlotinib as approximately twofold decreases in drug were observed in chronically compared to acutely treated mice, although no gender variation was observed (Compare Fig. 6a, c with Fig. 3a, b). In humans, the PK of erlotinib can be perturbed by chronic exposure to constituents in cigarettes. In the BR.21 clinical trial, current smoking lung cancer patients had median steady-state erlotinib trough plasma concentrations nearly half that of non-current smokers [50], and lower plasma levels of both erlotinib and OSI-420 were observed in smokers compared to non-smokers in healthy subjects [37]. This may occur through induction of enzymes that contribute to erlotinib metabolic clearance, including CYP1A1 and CYP1A2.

Gender differences in erlotinib PK were not been reported in cancer patients [51]. In a study of healthy male and female subjects, females achieved significantly greater exposure to erlotinib than males but gender variations in OSI-420 were not addressed [52]. In mice, the only publication evaluating erlotinib PK that we are aware of is the extensive report by Higgins et al. [53]. Our results on erlotinib PK in plasma from female mice are similar to this study, including the short plasma half-life of erlotinib in mice (1.5–4 h) compared to lung cancer patients (36 h) [51]. Other comparisons cannot be made, as the Higgins et al. study [53] was limited to plasma samples from non-tumor bearing, immunodeficient, female animals (*nu/nu*-nuBR nude athymic mice) and OSI-420 levels were not evaluated.

It seems unlikely that higher OSI-420 concentrations in males impacted tumor burden as OSI-420 levels were typically only 10–20% of erlotinib levels and both compounds are equally potent EGFR TKIs in vitro (data on file at OSI Pharmaceuticals). Similarly, OSI-420 plasma concentrations in humans account for only 5–10% of that of erlotinib [37]. Nonetheless, because of the correspondence between

elevated OSI-420 levels and male response, more extensive studies on gender differences in erlotinib metabolism may be informative, given the clinical implications, including that erlotinib is administered daily to lung cancer patients over prolonged periods of time.

One of the strengths of utilizing this primary lung cancer mouse model for erlotinib PK analysis is that drug levels can be directly measured in tumors to verify that biologically relevant levels are present. The amounts of erlotinib in tumors ranged from 2,000 to 3,500 ng/cm^3 (~5–9 μM) at peak levels to over 700 ng/g (2 μM) up to 4 h after erlotinib administration (Figs. 3c, 6b), well within the concentration range reported to inhibit sensitive human NSCLC cell lines (IC_{50} = 0.1–2 μM) [43, 44]. In fact, initial high levels of erlotinib (5–9 μM) may inhibit other targets in addition to EGFR, such as other ErbB family members. Interestingly, in both genders, erlotinib concentrations were twofold higher in tumors relative to adjacent UI lung tissue, and OSI-420 concentrated even more strongly in tumors (five to eightfold increase in tumors vs UI lung), as shown in Figs. 3 and 6. Tumors thus increase their uptake and/or decrease elimination of erlotinib and its metabolite compared to adjacent lung tissue, implying that the concentrations and/or activities of relevant metabolizing enzymes vary between normal and neoplastic lungs. We have previously shown reduced expression of cytochrome P450 enzymes in lung tumors relative to either whole lung tissue or precursor Clara cells, including CYP1A1 which is likely involved in lung metabolism of erlotinib [42, 54].

Gender differences in EGFR biology

To further understand the mechanistic basis for the male specific efficacy of erlotinib, the following aspects of EGFR-related biology were compared between male and female tumor-bearing mice: (1) *Kras* mutations, (2) *EGFR* mutations, (3) total EGFR levels, and (4) pEGFR levels.

The incidence of *Kras* codon 61 mutations was equally high between genders (~80%), as shown in Table 1, and thus does not appear to explain why tumors in females are resistant to erlotinib. However, more male tumors exhibited Q61R mutations relative to female tumors (Table 1), a gender distinction observed in erlotinib- and vehicle-treated mice which reflects a trend towards gender bias in tumor initiation. In previous mouse studies, the Q61R mutation associated with carcinomas while the Q61L corresponded to early-stage adenomas [46, 55]. These data, combined with the observed male response to erlotinib and greater tumor burden of males compared to females in Captisol-treated animals (Fig. 5), suggest that male tumors bearing the Q61R mutation have a more aggressive, faster growing phenotype with increased sensitivity to erlotinib. Most importantly, our results clearly show that tumors harboring *Kras* mutations in male mice shrink in response to erlotinib, indicating that *Kras* mutation and anti-EGFR TK activity are not necessarily mutually exclusive. Consistent with these findings, gefitinib decreased the size and number of lung lesions in a primary mouse model of lung cancer induced by conditional expression of mutant $Kras^{G12D}$ [56]. Another group reported resistance to erlotinib using the same transgenic model, but tumor burden was measured by MRI and histology and the authors stated that more sensitive measures of tumor size might reveal a partial response [57]; neither study indicated the gender of mice that were used.

A greater abundance of EGFR mutations in lung tumors in male mice did not explain their sensitivity to erlotinib as none were detected in exons 18–22 in either male or females treated either with erlotinib or Captisol vehicle. This is consistent with a *Kras*-driven mouse model of lung cancer, as tumors bearing *Kras* mutations rarely also have *EGFR* mutations [18, 19], possibly due to their overlapping signaling functions. While lung cancer patients bearing EGFR mutations are most likely to respond to EGFR TKIs, and in a few cases the responses are quite dramatic and long-lasting, it is also true that some patients with wild-type EGFR can benefit from this class of drugs [13, 21, 23]. A putative corollary of our data is the use of erlotinib for stage I lung cancer patients bearing early lung neoplasias that have wild-type EGFR if EGFR is highly phosphorylated.

The expression pattern and amount of total EGFR in tumors was similar between male and females as measured by immunohistochemistry (Fig. 7c, d) and immunoblotting (Fig. 8c), and these levels were not altered by erlotinib treatment (Figs. 7, 8). EGFR was also present in adjacent UI lung from both genders, with particularly high levels in the Clara cells lining the bronchioles (Figs. 7a, b, 8a, b), indicating that EGFR is not overexpressed in tumors relative to these normal lung cells. The lack of association between total EGFR levels and responsiveness is similar to the clinical setting, where the relationship between EGFR levels as detected by immunohistochemistry and clinical outcome with EGFR TKIs has been variable [4].

We did find, however, that the phosphorylation status of EGFR differed between genders. pEGFR levels were substantially greater in lung tumors from males as compared to females in Captisol-treated animals (Figs. 7i, j, 8c, d) and in adjacent UI lung tissue (Figs. 7g, h, 8a, b). pEGFR levels in male tumors decreased to a greater extent in response to erlotinib than in female tumors (Compare Fig. 7i, k vs j, l and Fig. 8c, d), providing a clear mechanism for the male specific efficacy of erlotinib in this model. There is surprisingly little information correlating phosphorylated wild-type EGFR with EGFR TKI sensitivity in preclinical studies or clinical trials given the numerous reports on other aspects of EGFR biology, such as total EGFR expression, EGFR

DNA copy number, EGFR mutations and downstream signaling [3, 4]. pEGFR was not detected in control tumors from a benzo(a)pyrene mouse model of lung cancer responsive to gefitinib as a chemopreventive agent [58]. This study was limited to female animals and therefore the inability to measure pEGFR is consistent with our data showing low levels of pEGFR in tumor samples from female mice. In clinical trials of EGFR TKIs, there are no reports of pEGFR levels before or after drug treatment [4], most likely due to the instability of pEGFR and the resulting technical difficulty of its assessment in archival human samples. Based on the data provided by our mouse studies showing the strong correspondence of pEGFR levels with tumor response, we propose that future efforts in EGFR TKI clinical trials should include measurement of pEGFR levels in lung tumors. We hypothesize that such pEGFR analyses in humans would facilitate identification of lung cancer patients likely to respond to EGFR TKIs.

The elevated levels of pEGFR in male compared to female tumors combined with the male-specific response to erlotinib, suggest that EGFR signaling plays a pivotal role in male mouse lung tumorgenesis. Tumor cells bearing activating EGFR mutations exhibit increased phosphorylation of EGFR and activation of downstream signaling in vitro [17]. This may promote dependency on a functional EGFR for survival in vivo, a phenomenon referred to as "oncogene addiction", providing a rationale for the exquisite sensitivity of tumors bearing EGFR mutations to erlotinib and gefitinib [17]. We hypothesize that male tumors in our mouse model are more dependent on EGFR signaling relative to female tumors. This should result in greater activation of signaling downstream from EGFR, including Ras/Raf/mitogen-activated protein kinase [extracellular signal-regulated kinase (ERK) 1/2], phosphatidylinositol 3-kinase (PI3K)/Akt, and signal transduction and activator of transcription (STAT) pathways. Increased EGFR signaling in male versus female tumors may also contribute to the higher tumor burden observed in control males compared to control females (Fig. 5). It is not known why pEGFR levels are higher in tumors and adjacent UI lung tissue from males compared to females. One intriguing explanation is that male mice are more aggressive than females and require more EGF to facilitate wound-healing. In fact, male mice contain tenfold more EGF compared to female mice in the submandibular glands that secrete EGF into saliva for application to wounds by licking [59]. Submandibular gland-derived EGF can also be found in the circulation and increased levels in males compared to females might enhance EGFR phosphorylation in multiple organs, including the lungs.

Altogether, these results show that erlotinib is an effective early chemotherapeutic in mouse lung tumors reliant on EGFR signaling. Clinically, the limited number of studies in early stages of lung cancer so far described have shown efficacy with EGFR TKIs [60]. The studies herein support further evaluation of this class of drugs as early chemotherapeutics or chemopreventive agents. The ongoing improvement of methods to detect lung cancer at initial stages of disease, including low-dose spiral computed tomography (CT), bronchoscopic evaluation of airways, and advanced techniques of sputum analysis [61], make the diagnosis and treatment of early lung cancer a realistic possibility for the future.

Acknowledgments We thank gratefully thank Mr. Ronald Hoffman for technical assistance with drug administration in the animal studies.

References

1. Parkin DM, Bray F, Ferlay J, Pisani P (2005) Global statistics, 2002. CA Cancer J Clin 55(2):74–108
2. American Cancer Society (2007) Cancer facts and figures 2007. American Cancer Society, Atlanta
3. Hirsch FR, Varella-Garcia M, Bunn PA, Di Maria MV, Veve R, Bremnes RM, Baron AE, Zeng C, Franklin WA (2003) Epidermal growth factor receptor in non-small-cell lung carcinomas: correlation between gene copy number and protein expression and impact on prognosis. J Clin Oncol 21:3798–3807
4. Arteaga CL (2002) Epidermal growth factor receptor dependence in human tumors: more than just expression? Oncologist 7(Suppl 4):31–39
5. Brabender J, Danenberg KD, Metzger R, Schneider PM, Park J, Salonga D, Holscher AH, Danenberg PV (2001) Epidermal growth factor receptor and HER2-neu mRNA expression in non-small cell lung cancer is correlated with survival. Clin Cancer Res 7:1850–1855
6. Yarden Y, Sliwkowski MX (2001) Untangling the ErbB signalling network. Nat Rev Mol Cell Biol 2:127–137
7. Jorissen RN, Walker F, Pouliot N, Garrett TP, Ward CW, Burgess AW (2003) Epidermal growth factor receptor: mechanisms of activation and signalling. Exp Cell Res 284:31–53
8. Pao W, Miller VA (2005) Epidermal growth factor receptor mutations, small-molecule kinase inhibitors, and non-small-cell lung cancer: current knowledge and future directions. J Clin Oncol 23:2556–2568
9. Hynes NE, Lane HA (2005) ERBB receptors and cancer: the complexity of targeted inhibitors. Nat Rev Cancer 5:341–354
10. Ono M, Kuwano M (2006) Molecular mechanisms of epidermal growth factor receptor (EGFR) activation and response to gefitinib and other EGFR-targeting drugs. Clin Cancer Res 12:7242–7251
11. Herbst RS, Bunn PA Jr (2006) Targeting the epidermal growth factor receptor in non-small cell lung cancer. Clin Cancer Res 9:5813–5824
12. Ciardiello F, De Vita F, Orditura M, Tortora G (2004) The role of EGFR inhibitors in non small cell lung cancer. Curr Opinion Oncol 16:130–135
13. Shepherd FA, Pereira JR, Ciuleanu T, Tan EH, Hirsh V, Thongprasert S, Campos D, Maoleekoonpiroj S, Smylie M, Martins R, van Kooten M, Dediu M, Findlay B, Tu DS, Johnston D, Bezjak A, Clark G, Santabarbara P, Seymour L (2005) Erlotinib in previously treated non-small-cell lung cancer. New Engl J Med 353:123–132
14. Kris MG, Natale RB, Herbst RS, Lynch TJ, Prager D, Belani CP, Schiller JH, Kelly K, Spiridonidis H, Sandler A, Albain KS, Cella

D, Wolf MK, Averbuch SD, Ochs JJ, Kay AC (2003) Efficacy of gefitinib, an inhibitor of the epidermal growth factor receptor tyrosine kinase, in symptomatic patients with non-small cell lung cancer—a randomized trial. JAMA 290:2149–2158
15. Lynch TJ, Bell DW, Sordella R, Gurubhagavatula S, Okimoto RA, Brannigan BW, Harris PL, Haserlat SM, Supko JG, Haluska FG, Louis DN, Christiani DC, Settleman J, Haber DA (2004) Activating mutations in the epidermal growth factor receptor underlying responsiveness of non-small-cell lung cancer to gefitinib. New Engl J Med 350:2129–2139
16. Paez JG, Janne PA, Lee JC, Tracy S, Greulich H, Gabriel S, Herman P, Kaye FJ, Lindeman N, Boggon TJ, Naoki K, Sasaki H, Fujii Y, Eck MJ, Sellers WR, Johnson BE, Meyerson M (2004) EGFR mutations in lung cancer: correlation with clinical response to gefitinib therapy. Science 304:1497–1500
17. Sharma SV, Bell DW, Settleman J, Haber DA (2007) Epidermal growth factor receptor mutations in lung cancer. Nat Rev Cancer 7:169–181
18. Pao W, Wang TY, Riely GJ, Miller VA, Pan QL, Ladanyi M, Zakowski MF, Heelan RT, Kris MG, Varmus HE (2005) KRAS mutations and primary resistance of lung adenocarcinomas to gefitinib or erlotinib. PLOS Med 2:57–61
19. Eberhard DA, Johnson BE, Amler LC, Goddard AD, Heldens SL, Herbst RS, Ince WL, Janne PA, Januario T, Johnson DH, Klein P, Miller VA, Ostland MA, Ramies DA, Sebisanovic D, Stinson JA, Zhang YR, Seshagiri S, Hillan KJ (2005) Mutations in the epidermal growth factor receptor and in KRAS are predictive and prognostic indicators in patients with non-small-cell lung cancer treated with chemotherapy alone and in combination with erlotinib. J Clin Oncol. 23:5900–5909
20. Cappuzzo F, Hirsch FR, Rossi E, Bartolini S, Ceresoli GL, Bemis L, Haney J, Witta S, Danenberg K, Domenichini I, Ludovini V, Magrini E, Gregorc V, Doglioni C, Sidoni A, Tonato M, Franklin WA, Crino L, Bunn PA Jr, Varella-Garcia M (2005) Epidermal growth factor receptor gene and protein and gefitinib sensitivity in non-small-cell lung cancer. J Natl Cancer Inst 97:643–655
21. Tsao MS, Sakurada A, Cutz JC, Zhu CQ, Kamel-Reid S, Squire J, Lorimer I, Zhang T, Liu N, Daneshmand M, Marrano P, da Cunha SG, Lagarde A, Richardson F, Seymour L, Whitehead M, Ding K, Pater J, Shepherd FA (2005) Erlotinib in lung cancer—molecular and clinical predictors of outcome. N Engl J Med 353:133–144
22. Pao W, Miller V, Zakowski M, Doherty J, Politi K, Sarkaria I, Singh B, Heelan R, Rusch V, Fulton L, Mardis E, Kupfer D, Wilson R, Kris M, Varmus H (2004) EGF receptor gene mutations are common in lung cancers from "never smokers" and are associated with sensitivity of tumors to gefitinib and erlotinib. PNAS 101:13306–13311
23. Bell DW, Lynch TJ, Haserlat SM, Harris PL, Okimoto RA, Brannigan BW, Sgroi DC, Muir B, Riemenschneider MJ, Iacona RB, Krebs AD, Johnson DH, Giaccone G, Herbst RS, Manegold C, Fukuoka M, Kris MG, Baselga J, Ochs JS, Haber DA (2005) Epidermal growth factor receptor mutations and gene amplification in non-small-cell lung cancer: molecular analysis of the IDEAL/INTACT gefitinib trials. J Clin Oncol 23:8081–8092
24. Rodenhuis S, Slebos RJ (1992) Clinical significance of ras oncogene activation in human lung cancer. Cancer Res 52:2665s–2669s
25. Mitsudomi T, Steinberg SM, Oie HK, Mulshine JL, Phelps R, Viallet J, Pass H, Minna JD, Gazdar AF (1991) Ras gene mutations in non-small cell lung cancers are associated with shortened survival irrespective of treatment intent. Cancer Res 51:4999–5002
26. Moore MJ, Goldstein D, Hamm J, Figer A, Hecht JR, Gallinger S, Au HJ, Murawa P, Walde D, Wolff RA, Campos D, Lim R, Ding K, Clark G, Voskoglou-Nomikos T, Ptasynski M, Parulekar W (2007) Erlotinib plus gemcitabine compared with gemcitabine alone in patients with advanced pancreatic cancer: a phase III trial of the National Cancer Institute of Canada Clin Trials Group. J Clin Oncol 25:1960–1966
27. Franklin WA, Veve R, Hirsch FR, Helfrich BA, Bunn PA Jr (2002) Epidermal growth factor receptor family in lung cancer and premalignancy. Sem Oncol 29:3–14
28. Merrick DT, Kittelson J, Winterhalder R, Kotantoulas G, Ingeberg S, Keith RL, Kennedy TC, Miller YE, Franklin WA, Hirsch FR (2006) Analysis of c-ErbB1/epidermal growth factor receptor and c-ErbB2/HER-2 expression in bronchial dysplasia: evaluation of potential targets for chemoprevention of lung cancer. Clin Cancer Res 12:2281–2288
29. Malkinson AM (1992) Primary lung tumors in mice: an experimentally manipulable model of human adenocarcinoma. Cancer Res 52:2670s–2676s
30. Malkinson AM (1998) Molecular comparison of human and mouse pulmonary adenocarcinomas. Exp Lung Res 24:541–555
31. Malkinson AM (2001) Primary lung tumors in mice as an aid for understanding, preventing, and treating human adenocarcinoma of the lung. Lung Cancer 32:265–279
32. O'Donnell EP, Zerbe LK, Dwyer-Nield LD, Kisley LR, Malkinson AM (2006) Quantitative analysis of early chemically-induced pulmonary lesions in mice of varying susceptibilities to lung tumorigenesis. Cancer Lett 241:197–202
33. Stearman RS, Dwyer-Nield L, Zerbe L, Blaine SA, Chan Z, Bunn PA Jr, Johnson GL, Hirsch FR, Merrick DT, Franklin WA, Baron AE, Keith RL, Nemenoff RA, Malkinson AM, Geraci MW (2005) Analysis of orthologous gene expression between human pulmonary adenocarcinoma and a carcinogen-induced murine model. Am J Pathol 167:1763–1775
34. Sweet-Cordero A, Tseng GC, You H, Douglass M, Huey B, Albertson D, Jacks T (2006) Comparison of gene expression and DNA copy number changes in a murine model of lung cancer. Genes Chromosomes Cancer 45:338–348
35. Fisher GH, Wellen SL, Klimstra D, Lenczowski JM, Tichelaar JW, Lizak MJ, Whitsett JA, Koretsky A, Varmus HE (2001) Induction and apoptotic regression of lung adenocarcinomas by regulation of a K-Ras transgene in the presence and absence of tumor suppressor genes. Genes Dev 15:3249–3262
36. Johnson L, Mercer K, Greenbaum D, Bronson RT, Crowley D, Tuveson DA, Jacks T (2001) Somatic activation of the K-ras oncogene causes early onset lung cancer in mice. Nature 410:1111–1116
37. Hamilton M, Wolf JL, Rusk J, Beard SE, Clark GM, Witt K, Cagnoni PJ (2006) Effects of smoking on the pharmacokinetics of erlotinib. Clin Cancer Res 12:2166–2171
38. Malkinson AM, Beer DS (1983) Major effect on susceptibility to urethan-induced pulmonary adenoma by a single gene in BALB/cBy mice. J Natl Cancer Inst 70:931–936
39. McRae G, Lazaro L, Liao L, Papadopoulos P, Osdon M (2002) Validation of a high performance liquid chromatographic method for the determination of OSI-774 and OSI-420 in human plasma (heparin) specific to OSI Pharmaceuticals. MDS Pharma Services, Montreal
40. Conklin E, Hamilton M, Drolet D, Keatly K, Tucker C (2004) Method protocol and corresponding validation report for the quantification of OSI-774 and major metabolite OSI-420/413 in human EDTA plasma by HPLC/MS/MS. OSI Pharmaceuticals IBC, assignee
41. Lowry OH, Rosebrough NJ, Farr AL, Randall RJ (1951) Protein measurement with the folin phenol reagent. J Biol Chem 193:265–275
42. Ling J, Johnson KA, Miao Z, Rakhit A, Pantze MP, Hamilton M, Lum BL, Prakash C (2006) Metabolism and excretion of erlotinib, a small molecule inhibitor of epidermal growth factor receptor tyrosine kinase, in healthy male volunteers. Drug Metab Dispos 34:420–426

43. Thomson S, Buck E, Petti F, Griffin G, Brown E, Ramnarine N, Iwata KK, Gibson N, Haley JD (2005) Epithelial to mesenchymal transition is a determinant of sensitivity of non-small-cell lung carcinoma cell lines and xenografts to epidermal growth factor receptor inhibition. Cancer Res 65:9455–9462
44. Yauch RL, Januario T, Eberhard DA, Cavet G, Zhu W, Fu L, Pham TQ, Soriano R, Stinson J, Seshagiri S, Modrusan Z, Lin C, O-Neill V, Amler LC (2005) Epithelial versus mesenchymal phenotype determines in vitro sensitivity and predicts clinical activity of erlotinib in lung cancer patients. Clin Cancer Res 11:8686–8698
45. You M, Candrian U, Maronpot RR, Stoner GD, Anderson MW (1989) Activation of the Ki-ras protooncogene in spontaneously occurring and chemically induced lung tumors of the strain A mouse. PNAS 86:3070–3074
46. Nuzum EO, Malkinson AM, Beer DG (1990) Specific ki-ras codon-61 mutations may determine the development of urethane-induced mouse lung adenomas or adenocarcinomas. Molec Carcinog 3:287–295
47. Malumbres M, Barbacid M (2003) RAS oncogenes: the first 30 years. Nat Rev Cancer 3:459–465
48. Jorissen RN, Walker F, Pouliot N, Garrett TPJ, Ward CW, Burgess AW (2003) Epidermal growth factor receptor:mechanisms of activation and signalling. Exp Cell Res 284:31–53
49. Van Winkle LS, Gunderson AD, Shimizu JA, Baker GL, Brown CD (2002) Gender differences in naphthalene metabolism and naphthalene-induced acute lung injury. Am J Physiol Lung Cell Molec Physiol 282:L1122–L1134
50. Hamilton M, Wolf JL, Zborowski D, Lu J, Lum BL, Ding K, Clark GM, Rakhit A, Seymour L, Ptaszynski AM, Rusk J, Shepherd F (2005) Tarceva (erlotinib) exposure/effects (EE) analysis from a phase III study in advanced NSCLC. Effect of smoking on the PK of erlotinib. Proc Am Assoc Cancer Res 46:1451
51. Tarceva [prescribing information] (2005) Genentech, Melville, NY. Am Cancer Society 52:23–47
52. Frohna P, Lu J, Eppler S, Hamilton M, Wolf J, Rakhit A, Ling J, Kenkare-Mitra SR, Lum BL (2006) Evaluation of the absolute oral bioavailability and bioequivalence of erlotinib, an inhibitor of the epidermal growth factor receptor tyrosine kinase, in a randomized, crossover study in healthy subjects. J Clin Pharmacol 46:282–290
53. Higgins B, Kolinsky K, Smith M, Beck G, Rashed M, Adames V, Linn M, Wheeldon E, Gand L, Birnboeck H, Hoffmann G (2004) Antitumor activity of erlotinib (OSI-774, Tarceva) alone or in combination in human non-small cell lung cancer tumor xenograft models. Anti-Cancer Drugs 15:503–512
54. Forkert PG, Parkinson A, Thaete LG, Malkinson AM (1992) Resistance of murine lung-tumors to xenobiotic-induced cytotoxicity. Cancer Res 52:6797–6803
55. Gressani KM, Leone-Kabler S, O'Sullivan MG, Case LD, Malkinson AM, Miller MS (1999) Strain-dependent lung tumor formation in mice transplacentally exposed to 3-methylcholanthrene and post-natally exposed to butylated hydroxytoluene. Carcinogenesis 20:2159–2165
56. Fujimoto N, Wislez M, Zhang J, Iwanaga K, Dackor J, Hanna AE, Kalyankrishna S, Cody DD, Price RE, Sato M, Shay JW, Minna JD, Peyton M, Tang X, Massarelli E, Herbst R, Threadgill DW, Wistuba II, Kurie JM (2005) High expression of ErbB family members and their ligands in lung adenocarcinomas that are sensitive to inhibition of epidermal growth factor receptor. Cancer Res 65:11478–11485
57. Politi K, Zakowski MF, Fan PD, Schonfeld EA, Pao W, Varmus HE (2006) Lung adenocarcinomas induced in mice by mutant EGF receptors found in human lung cancers respond to a tyrosine kinase inhibitor or to down-regulation of the receptors. Genes Develop 20:1496–1510
58. Yan Y, Lu Y, Wang M, Vikis H, Yao R, Wang Y, Lubet RA, You M (2006) Effect of an epidermal growth factor receptor inhibitor in mouse models of lung cancer. Mol Cancer Res 4:971–981
59. Barka T (1980) Biologically active polypeptides in submandibular glands. J Histochem Cytochem 28:836–859
60. Potti A, Ganti AK (2006) Adjuvant chemotherapy for early-stage non-small cell lung cancer: the past, the present and the future. Expert Opin Biol Ther 6:709–716
61. Ashton RW, Jett JR (2005) Screening for non-small cell lung cancer. Semin Oncol 32:253–258